TRANSPORT PROBLEMS 2023 Volume 18 Issue 4
PROBLEMY TRANSPORTU DOI: 10.20858/tp.2023.18.4.13

Keywords: vibration damper; torsional vibrations; temperature; saturation time

Wojciech HOMIK[1], Aleksander MAZURKOW[2], Andrzej CHMIELOWIEC[3]*

DETERMINATION OF A TORSIONAL VIBRATION VISCOUS DAMPER'S OPERATING TEMPERATURE USING A NEW THERMOHYDRODYNAMIC MODEL

Summary. This article presents an innovative algorithm and mathematical model of a torsional vibration viscous damper. The problem of torsional vibrations damping in a multicylinder internal combustion engine is extremely important for the reliable operation of a drive unit. The effective reduction of the vibration amplitude extends the service life and prevents failures that generate logistic and transport problems. One of the key parameters used to assess the quality of vibration damper operation is the temperature. This criterion is so important that it is the main indicator for the possible replacement of dampers installed in trucks, locomotives, and ships. Despite the importance of this parameter, the literature lacks mathematical models that describe the thermodynamics of damper operation. Therefore, the authors of this paper developed and presented an innovative thermohydrodynamic model of a torsional vibrations viscous damper, which was used to determine the operating parameters.

1. INTRODUCTION

One of the transportation problems is ensuring the reliable operation of propulsion systems. The reciprocating internal combustion engine is a source of vibroacoustic phenomena, which pose a serious threat to the fatigue strength of a propulsion system. They result from the action of periodically variable forces on the piston-crankshaft system of the engine: gas pressure and inertial forces. Regardless of the dynamic system in which the engine operates, the greatest threat to its components, especially the crankshaft, is torsional vibrations. Torsional vibration dampers are used to minimize this risk. They are most commonly placed on the end of the engine's crankshaft. Torsional vibration viscous dampers are widely used in the propulsion systems of automobiles, construction machinery, diesel locomotives, and marine vessels. They are individually designed for a specific type of engine, taking into account the complexity of the entire propulsion system based on discrete models (Fig. 1).

As evidenced in practice, these models provide a reasonable approximation to reality, but they do not allow for the analysis of phenomena such as thermohydrodynamic effects accompanying the operation of a damping device. With this in mind, the authors proposed an innovative model of a passive torsional vibration viscous damper.

[1] Rzeszow University of Technology, The Faculty of Mechanical Engineering and Aeronautics, Powstancow Warszawy 12, 35-959 Rzeszow, Poland, whomik@prz.edu.pl; orcid.org/0000-0001-7843-7761
[2] Rzeszow University of Technology, The Faculty of Mechanical Engineering and Aeronautics, Powstancow Warszawy 12, 35-959 Rzeszow, Poland, almaz@prz.edu.pl; orcid.org/0000-0003-1719-991X
[3] Rzeszow University of Technology, The Faculty of Mechanics and Technology, Kwiatkowskiego 4, 37-450 Stalowa Wola, Poland, achmie@prz.edu.pl; orcid.org/0000-0001-6629-0029
* Corresponding author. E-mail: achmie@prz.edu.pl

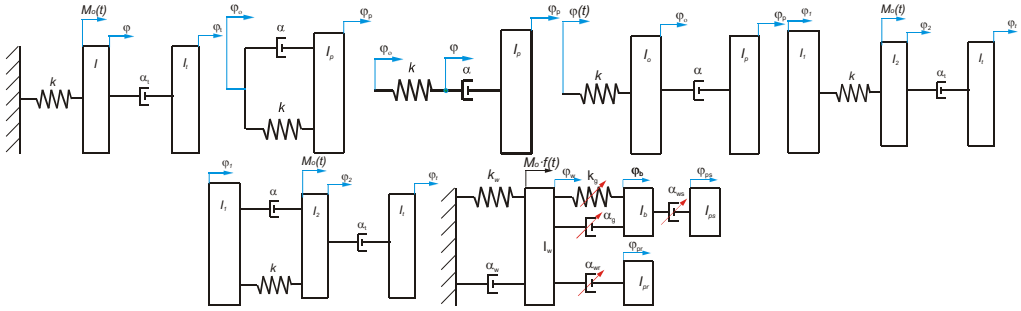

Fig. 1. Examples of damping modeling

Despite the fulfillment of many criteria regarding the material structure, strength, and design rules [1, 2], crankshafts are still emergency elements. Damage occurs regardless of their application. They are present in compressors [3], trucks [4], buses [5], and even airplanes [6]. Many authors have analyzed failure examples to draw appropriate conclusions for the future [7-9]. Global databases are being created to collect information about failures around the world [10]. Increasingly accurate methods for monitoring the condition of crankshafts and warning against their failure have been introduced [11-15].

The utilization of a torsional vibration viscous damper is one way to prolong the reliable operational lifespan of a crankshaft [16-18]. For large marine engines, special torsional vibration assessment procedures have been proposed [19]. Nonetheless, many publications addressing multi-cylinder internal combustion engines extensively discuss topics such as engine design, ignition methods, power supply and cooling system structures, piston and crank mechanisms, the materials employed in engine component fabrication, and the comprehensive approach to designing specific engine parts. On the other hand, the phenomena that accompany a running engine are described marginally. In many cases, these phenomena significantly affect the reliability, durability, and vibroacoustic effects of an engine. One area that has received limited attention is the issue of crankshaft torsional vibrations and strategies for mitigating them. This might be attributed to the notion that torsional vibrations are not as significant a threat to crankshafts as bending or longitudinal vibrations. The exceptions are the studies [18, 20-21].

Undoubtedly, the most difficult-to-detect crankshaft vibrations are torsional vibrations. The main reason for this is the fact that they overlap with the rotational motion and do not cause additional vibroacoustic phenomena. Very often, these vibrations are wrongly attributed to other phenomena accompanying the rotation of the shaft. Therefore, we try to eliminate them by inappropriate methods. The misinterpretation of this phenomenon often comes to light in the case of the drive system serious failure (e.g., damage of the shaft) (Fig. 2).

Fig. 2. A damaged shaft

A range of techniques has been employed to eradicate torsional vibrations and their consequences. One possibility is to use a device called a vibration damper. Currently, there are many design solutions available for this type of device. One of the most commonly used solutions is the application of torsional vibrations viscous dampers. They are currently used in the propulsion systems of ships, diesel locomotives, working machines, buses, and trucks.

Torsional vibrations viscous dampers' simple structure (Fig. 3) and relatively long service life have undoubtedly contributed to their great popularity. Furthermore, their effectiveness across the entire spectrum of engine rotational speeds is crucial when compared to alternative design solutions. This characteristic enables the engine to transition relatively seamlessly through what is known as critical speeds. The graph in Fig. 4 shows the amplitude values of the crankshaft vibrations for different rotational speeds and different types of dampers. The graph clearly shows that silicone dampers (silicone Torsional Vibrations Damper (TVD)) and silicone-rubber dampers (silicone-rubber TVD) significantly reduce the vibrations' amplitude for all the tested rotational speeds. When the engine is working without a damper (without TVD) or with a rubber damper (rubber TVD), we can observe certain frequencies for which the amplitude of vibrations significantly increases.

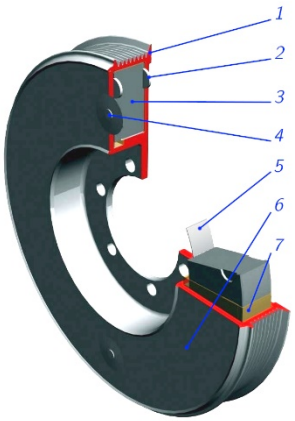

Fig. 3. Torsional vibrations viscous damper: 1 - damper housing, 2 - thrust bearing, 3 - inertia ring, 4 - plug, 5 - radial bearing, 6 - cover, 7 - silicone oil

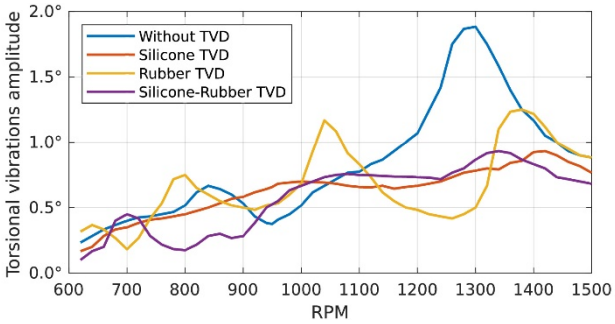

Fig. 4. Torsional vibrations' amplitudes of the shaft without a torsional vibrations damper (TVD) and with different types of torsional vibrations dampers [22]

2. VIBRATION DAMPING

Torsional vibrations in shafts are typically subtle and inconspicuous, but they can also generate unwanted noise. This occurs when the engine operates within the realm of resonant rotational speeds or in cases in which the damper is compromised (see Fig. 5) or chosen incorrectly.

(a) (b) (c)

Fig. 5. Mechanical damage to the active surfaces of a torsional vibrations viscous damper

The torsional vibrations of crankshafts were first noticed in the shipbuilding industry in the 1920s. At that time, the first naval unit equipped with a torsional vibrations viscous damper was a submarine's engine. The damper has been installed to extend the life of the propulsion system, reduce vibrations that generate acoustic waves, and improve crew comfort [23-25].

If a properly sized and technically efficient damper is fitted to the drive unit (engine), then ship crews, working machine operators, and drivers should not feel the nuisance vibroacoustic phenomena during work.

The users of the drive units do not influence the selection of the appropriate damper but are responsible for maintaining it in a proper technical condition and taking care of its reliability. The authors of the article, during the research conducted in a company dealing with diagnostics, regeneration, and repair of torsional vibrations dampers, noticed that the technical condition of the damper is not the subject of engine users' attention. There are several basic reasons for this:

- it is difficult to access the damper,
- it is impossible to take a silicone oil sample for testing,
- it is impossible to prepare the engine crankshaft amplitude-frequency characteristics and compare them with reference values.

The presented problems became the starting point for the search for new methods of diagnosing the technical condition of torsional vibrations viscous dampers. Cooperation with the aforementioned company resulted in the invention of criteria for evaluating the efficiency of torsional vibrations viscous dampers. One of them is the thermal criterion, which consists of measuring the time when the damper reaches the saturation temperature.

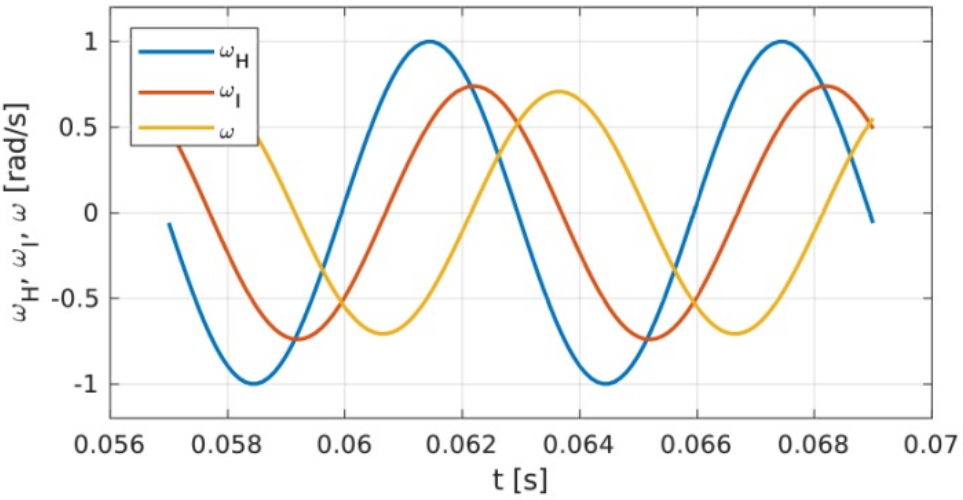

Fig. 6. Diagrams of angular velocities: ω_H (housing angular velocity), ω_I (inertia ring angular velocity), $\omega = \omega_I - \omega_H$ (relative angular velocity) [22]

As mentioned earlier, the primary function of the damper is to effectively reduce the torsional vibrations of the shaft and any associated vibroacoustic consequences. Extensive years of research and theoretical investigation have revealed that the motion of the damper's inertia ring concerning its housing commences when the torsional vibration amplitude of the shaft exceeds a specific threshold. This relative motion occurrence (Fig. 6) reduces the amplitude of the shaft's torsional vibrations, causing the damper to convert mechanical energy into heat and leading the damper housing to heat up. The diagram in Fig. 6 shows the angular velocity of the housing ω_H, as well as the angular velocity of the inertia ring ω_I, measured on the test stand after setting the damper to oscillate. The relative angular velocity $\omega = \omega_I - \omega_H$ causes frictional forces inside the oil, filling the damper. As a result, we obtain a mechanism that dissipates the energy of torsional vibrations. It should be noted that under real conditions, the oscillations are performed around a certain mean, non-zero angular velocity. This can be graphically represented by an appropriate vertical shift of the plot.

3. WORKING TEMPERATURE OF A VIBRATIONS DAMPER

During the beginning phase of the damper's use, the heat it generates causes it to warm up, and some of this heat is released into the surrounding environment. As the temperature rises, more heat is transferred to the outside. This pattern persists until an equilibrium is achieved between the produced heat and the heat released into the environment. The time it takes for the damper to reach this equilibrium, referred to as the damper saturation time, can serve as a metric for the damper's efficiency.

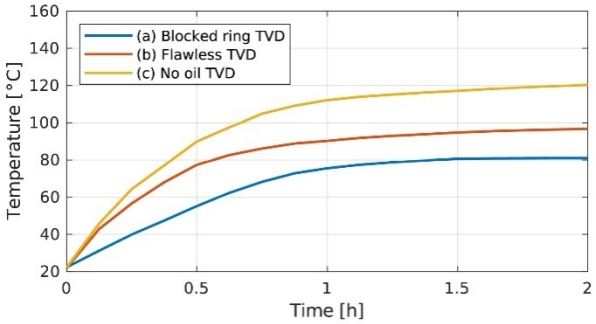

Fig. 7. Changes in the torsional vibrations damper (TVD) temperature as a function of time: a) a TVD with a blocked inertia ring, b) a flawless TVD, and c) a TVD without oil [22]

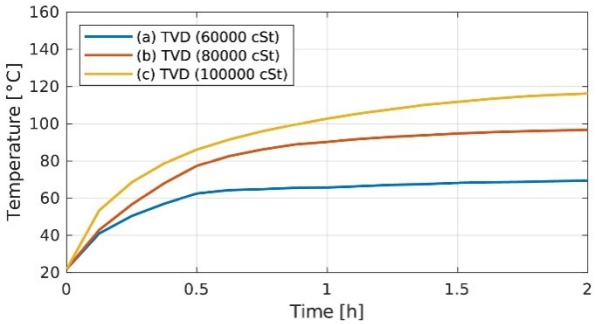

Fig. 8. Variations in temperature over time for a torsional vibrations damper (TVD) containing fluids with varying viscosities [22]

The time it takes for the damper to reach equilibrium, known as the damper saturation time, is not a fixed value and is influenced by various factors such as the damper's technical state, size, the viscosity of the liquid it contains, the speed at which the shaft rotates, the level of vibrations, and the operating environment. The graph in Fig. 7 shows the rate of the damper temperature rise in cases of a locked inertia ring, a properly functioning damper, and a damper without silicone oil [26]. In the first case, internal friction forces cause a lower temperature increase than in the case of a properly functioning damper. This is because the locking of the inertia ring usually occurs as a result of changing the silicone oil state from liquid to gel. In this situation, the characteristics of the damper are more like a rubber damper than a silicone viscous damper. As a result, the efficiency of dissipating the vibrations of the crankshaft is worse. In the absence of oil, however, there is dry friction between the inertia ring and the housing. This results in the overheating of the damper and the drastic wear of the rubbing surfaces.

The graph in Fig. 8 shows the change in the damper temperature as a function of time for different silicone oil viscosity values. It can be seen that the higher the viscosity, the higher the temperature. A careful analysis of the graph shows that this increase is not linear. Therefore, for sufficiently high viscosities, the blocking of the ring and a drop in temperature should be expected due to the negligible relative movement of the housing and the ring. It should be emphasized that the previous statement is the only hypothesis of the authors, who do not yet have full experimental results in this regard.

The presented examples show that the measurement of the damper's saturation time, or even its temperature, gives information about the damper's technical condition. For example, the results presented in Fig. 7 allow us to determine the condition of the oil. Based on the damper heating rate in

time, we can conclude that the oil is deficient c) or that the oil turns into gel a). The analysis of the results indicates that in some cases, the temperature of a technically inoperative damper may exceed the permissible values during engine operation (e.g., a damper operating without oil – Fig. 7, curve c). Permissible temperatures are those that do not cause such a flow of thermal energy that the damper is damaged. In such a situation, overheating occurs most often, and its consequence is damper seizure [27]. Failure to reach the appropriate temperature is most likely a signal that the oil has turned to gel and the damper is blocked (Fig. 7, curve c).

In practice, there are effective methods to protect the damper from overheating. Nevertheless, it is important to know that they increase the cost of installation and complicate its construction. In practice, the phenomenon of the overheating and seizure of the damper causes the device to excite the vibrations instead of damping them.

A properly designed damper should work without failure for a period of 20,000 to 30,000 hours, in the temperature range from $-30°C$ to even $120°C$. Laboratory tests conducted by the authors in cooperation with the mentioned company have shown that the damper seizure occurs when its operating temperature exceeds the temperature for which it was designed by $60°C$.

Satisfactory results of the damper's work are achieved when it works in the temperature range of $75°C$ to $90°C$. The maximum allowable heat transfer rate in the damper depends on:

- operating conditions (including engine rotational speed),
- the size of the damper,
- damper's structure (bolted damper housing, rolled damper housing).

Its value is expressed by the following general formula:

$$\dot{Q} = \dot{q} \cdot A_{\mathrm{p}}, \tag{1}$$

where $\dot{Q}$ denotes the maximum allowable heat transfer rate in W, A_{p} is the total area of the inertia ring in m^2, and $\dot{q}$ is the experimentally determined maximum heat flux density that the damper is able to dissipate. According to [28], the maximum values are as follows: $\dot{q} = 5\,000 \div 6\,100$ $\mathrm{W{\cdot}m^{-2}}$ for temporary work at the critical angular velocity, $\dot{q} = 2\,500 \div 3\,050$ $\mathrm{W{\cdot}m^{-2}}$ for dampers in small engines with a high angular velocity, such as those used in cars and designed for continuous operation at critical angular velocity, and $\dot{q} = 1\,250 \div 1\,525$ $\mathrm{W{\cdot}m^{-2}}$ for dampers in large engines with a small angular velocity, such as those used in ships, and designed for continuous operation at critical angular velocity.

Understanding the importance of the above problem, the authors of this publication decided to develop a thermohydrodynamic computational model of a torsional vibrations viscous damper, which would enable the determination of the correct operating temperature range.

4. MODEL OF A TORSIONAL VIBRATIONS VISCOUS DAMPER

Later in the article, we assume that the notation $X_i, X_{*,i}$ means $X_1, X_{*,1}$ or $X_2, X_{*,2}$, respectively, where $X_1, X_{*,1}$ refers to the value related to the inner oil gap and $X_2, X_{*,2}$ refers to the value related to the outer oil gap. We suggest such indices because both gaps are governed by analogous thermo-hydrodynamic laws, and the difference comes down to the geometric dimensions and oil flow velocity. Fig. 9 describes the basic geometric parameters of a torsional vibrations viscous damper.

The mentioned geometrical parameters and material properties determine the moment of inertia of the ring. They also directly affect the value of the frictional moment and damping value, which directly transforms into the amount of energy dissipated by the damper. In addition to the above-mentioned geometric parameters, the following factors have a decisive influence on its work:

- inner radial clearance $C_1 = R_{I,1} - R_{H,1}$,
- outer radial clearance $C_2 = R_{H,2} - R_{I,2}$.

When the damper reaches its saturation temperature and thus starts to operate in a steady state, two oil films are formed between the damper housing and its inertia ring: inner and outer. The oil films create the internal and external hydrodynamic forces F_{L1} and F_{L2}, balancing the inertia ring weight F and enabling it to be lifted.

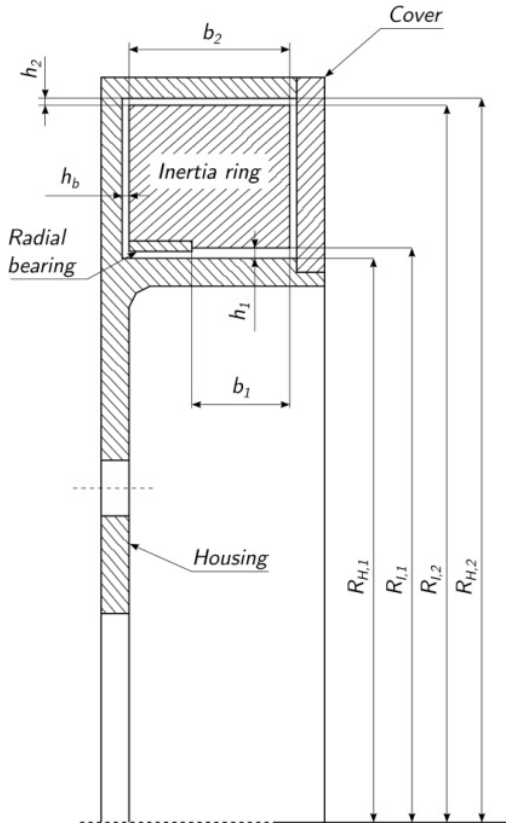

$R_{H,1}$ – housing inner radius
$R_{I,1}$ – inertia ring inner radius
$R_{I,2}$ – inertia ring outer radius
$R_{H,2}$ – housing outer radius
b_1, b_2 – inner and outer widths of the inertia ring
h_1, h_2 – inner and outer oil film thicknesses
h_b – front oil film thicknesses

Fig. 9. Description of the fundamental geometric characteristics of the damper.

The oil layer velocity in the circumferential direction (Fig. 10) depends on the ring angular velocity in relation to the housing angular velocity $\omega = \omega_I - \omega_H$. On the other hand, the oil flow in the axial direction results from the pressure difference between the oil film $p(\varphi, z)$ and the pressure in the damper front space p_0. In order to simplify the model, the authors also assumed that the damper was not equipped with a radial bearing. Therefore, it was omitted in Fig. 10, and it was assumed that $b_1 = b_2$. Note that this assumption does not reduce the generality of the model. This is because one can *cut* the inertia ring into two widths, b_1 and $b_2 - b_1$, if there is a need to take into account a radial bearing.

In the steady state, under liquid friction conditions, the damper operation is described by the following quantities:

- the relative eccentricity of the inner and outer oil film
$$\varepsilon_i = \frac{e_i}{C_i}, \qquad e = e_1 = e_2, \tag{2}$$
- the Sommerfeld number defined according to the standard [29] for the inner and outer oil film
$$S_{0,i} = \frac{F \cdot \psi_i^2}{b_i \cdot D_i \cdot \eta \cdot \omega}, \tag{3}$$
where $\psi_i = C_i/R_{H,i}$, $D_i = 2R_{H,i}$, and η is the dynamic viscosity of the silicone oil. At this point, it should be noted that the difference between $R_{H,i}$ and $R_{I,i}$ in a real damper is so small that, for the purposes of the model, one can also assume $\psi_i = C_i/R_{I,i}$ and $D_i = 2R_{I,i}$, F is the weight of the inertia ring balanced by the hydrodynamic force and satisfies the condition $F = F_L = F_{L1} + F_{L2}$,
- housing temperature T_B,
- the minimum height of the inner and outer oil film $h_{\min,1}$ and $h_{\min,2}$,
- the average pressure of internal and external oil film $p_{\mathrm{m},1} = F_{L1}/(b_1 D_{I,1})$ and $p_{\mathrm{m},2} = F_{L2}/(b_2 D_{H,2})$.

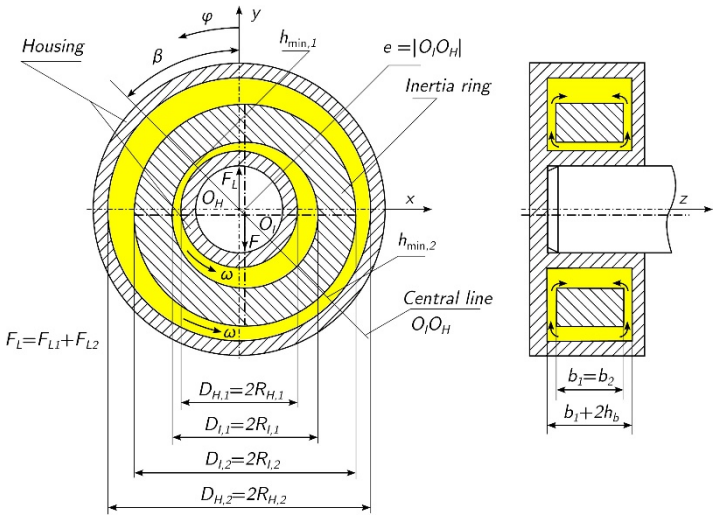

Fig. 10. Geometry, oil flow directions, and forces occurring in a torsional vibrations viscous damper

The assumptions for the thermohydrodynamic model of the torsional vibrations viscous damper are related to:

1. damper construction elements:
   a. construction elements are non-deformable, perfectly smooth, axial parallel and cylindrical surfaces,
   b. the inertia ring material is homogeneous,
2. oil properties:
   a. the oil is an incompressible Newtonian fluid within the range of simulated temperatures and operating shear rates,
   b. the oil viscosity is a function of temperature and is described by the relationship $\eta = \eta(T)$,
   c. the pressure generated in the oil film may take values greater than or equal to zero,
   d. the pressure in the direction of the radial variable y is constant,
   e. the ambient pressure is constant,
3. oil flow:
   a. the flow is laminar for $\mathrm{Re}_i = \frac{\rho \cdot \omega \cdot D_i \cdot C_i}{4\eta} \leq \mathrm{Re}_{i,\mathrm{CR}} \approx \frac{41.3}{\sqrt{\psi_i}}$ [29],
   b. the velocity of the oil film near the surface is equal to the velocity of the surface rotating inertia ring or housing,
   c. the oil flow rate in the axial direction is much greater than the flow rate of the oil flowing in the circumferential direction (according to [30], such an assumption is perfectly justified in the case of small angular velocity, and such is the relative velocity ω of the housing and the inertia ring),
4. heat generation:
   a. the heat generated by the frictional forces is used to change the enthalpy,
   b. ambient temperature $T_z = \text{const.}$,
   c. fluid heat exchange takes place by convection [30-34],
   d. in the vicinity of the housing, heat is absorbed by conduction through the damper housing and discharged to the environment,
   e. the heat transfer coefficient α $\mathrm{W{\cdot}m^{-2}{\cdot}K^{-1}}$ is assumed to be constant (this article assumes the value $\alpha = 20$ $\mathrm{W{\cdot}m^{-2}{\cdot}K^{-1}}$, which is in accordance with the standard [29], which determines the value of this coefficient for a steel cylindrical shape in the range of $15 \div 20$ $\mathrm{W{\cdot}m^{-2}{\cdot}K^{-1}}$).

Let us note here that the assumption of the laminarity of the silicone oil flow is crucial for the model presented in this article. From condition 3 a) for flow laminarity, the value of the Reynolds number can be determined for both the inner and outer gaps. For the damper that was used as an example, we have:

1. $D_1 = 0.157$ m, $C_1 = 0.14 \cdot 10^{-3}$ m, $\psi_1 = 2C_1/D_1 = 1.78 \cdot 10^{-3}$, $\rho = 970$ kg·m^{-3}, $\omega_{\max} = 2$ rad·s^{-1}, $\eta_{\min} = 10$ Pa·s, which, for the internal oil gap, gives a value of the Reynolds number equal to $\mathrm{Re}_1 \approx 10^{-3}$ and $\mathrm{Re}_{1,\mathrm{CR}} \approx 978.9$,
2. $D_2 = 0.26$ m, $C_2 = 0.52 \cdot 10^{-3}$ m, $\psi_2 = 2C_2/D_2 = 2 \cdot 10^{-3}$, $\rho = 970$ kg·m^{-3}, $\omega_{\max} = 2$ rad·s^{-1}, $\eta_{\min} = 10$ Pa·s, which, for the internal oil gap, gives a value of the Reynolds number equal to $\mathrm{Re}_2 \approx 6.5 \cdot 10^{-3}$ and $\mathrm{Re}_{2,\mathrm{CR}} \approx 923.5$.

The above calculations clearly show that $\mathrm{Re}_i < \mathrm{Re}_{i,\mathrm{CR}}$, which indicates flow laminarity in both gaps of the analyzed damper.

The mathematical model of a torsional vibrations viscous damper with heat dissipation through the housing has been described by a system of equations that include:

- the shape of the lubrication gap,
- pressure distribution in the lubricating gap,
- temperature distribution in the oil film when the heat from the damper is carried away by the flowing oil,
- the thermophysical properties of silicone oil.

For the damper geometry presented above (Fig. 10), the height of the oil film is a function of relative eccentricity. Let us assume that the angle of the ring center and the housing center is measured from the load direction. In this case, the height of the oil film is given by the following formula:

$$h_i = C_i(1 + \varepsilon_i \cos\varphi). \tag{4}$$

The pressure distribution in the viscous damper was derived from the Navier-Stokes equation and the equation of the continuity of fluid flow. After the appropriate transformations for the assumed fluid flow conditions in the damper are applied, the pressure distribution equation takes the following form:

$$\frac{\partial}{\partial z}\left(h_i^3 \frac{\partial p_i}{\partial z}\right) = 6\eta\omega \frac{\partial h_i}{\partial \varphi}. \tag{5}$$

As already mentioned, the thermal energy generated by the frictional forces $P_\mathrm{f} = \frac{1}{2}\omega f F_L D_2$ is discharged into the environment through the housing. Based on the assumptions made earlier, this temperature is expressed by the following relationship:

$$T_\mathrm{B} = T_0 + \frac{\omega f F_L D_2}{2\alpha A_\mathrm{B}}, \tag{6}$$

where T_B is the damper housing temperature taking into account the results of the bench tests, for which the condition for the correct operation of the damper was defined as $T_\mathrm{B} \leq 90$°C [35], T_0 is the ambient temperature, A_B is heat dissipation area, α is a value of the heat transfer coefficient, and f is the fluid friction coefficient [29, 34].

Viscosity is a fundamental thermophysical quantity that describes the phenomenon of internal friction caused by the resistance of oil as one layer moves relative to another. A distinction is made between kinematic viscosity ν and dynamic viscosity η. The kinematic viscosity ν of silicone oils used in torsional vibrations viscous dampers can be described by the following relationship:

$$\log\big(\nu(T)\big) = \frac{793.1}{273.0 + T} - 2.559 + \log\big(\nu(T_{25})\big), \tag{7}$$

for T ranging from 25°C to 250°C. The dynamic viscosity η can be expressed by the following relationship [35, 36]:

$$\eta(T) = \rho \cdot \nu(T), \tag{8}$$

where $\rho = 970$ kg/m^3. The graph of dynamic viscosity as a function of temperature for M30000 oil is shown in Fig. 11.

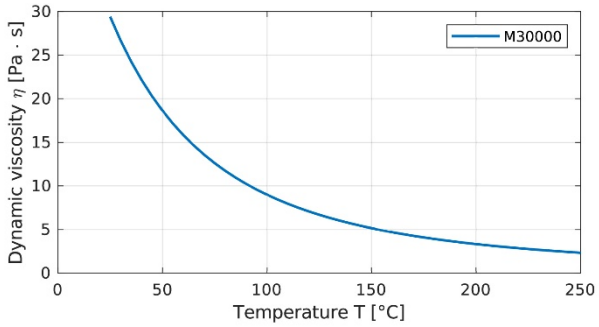

Fig. 11. Silicone oil M30000 dynamic viscosity as a function of temperature

5. TEMPERATURE SIMULATION OF THE WORKING TORSIONAL VIBRATIONS VISCOUS DAMPER

The operating temperature of the torsional vibrations viscous damper was calculated for the geometry and data presented in Table 1. It was assumed that the damper was filled with M30000 silicone oil and the weight of its inertia ring was $F = 89.6$ N.

The algorithm for solving the system of equations presented in the previous section is shown in the form of a network diagram in Fig. 12.

Table 1

Simulation parameters

Parameters of a torsional vibrations viscous damper	
1. The inner radius of the inertia ring	$R_{I,1} = 78.5$ mm
2. The outer radius of the housing interior	$R_{H,2} = 130$ mm
3. Inner radial clearance	$C_1 \in \{0.04, 0.14\}$ mm
4. Outer radial clearance	$C_2 \in \{0.475, 0.52\}$ mm
5. Width of the inertia ring	$b_1 = b_2 = 33$ mm
6. External surface of the damper	$A_B = 0.128$ m^2
7. Weight of the inertia ring	$F = 89.6$ N
8. The heat transfer coefficient	$\alpha = 20$ W·m^{-2} ·K^{-1}
The remaining input values for the calculation of the damper operating parameters	
9. Type of silicone oil	M30000
10. Silicone oil dynamic viscosity function	$\eta(T)$ computed from (7) and (8)
11. Silicone oil density	$\rho = 970$ kg·m^{-3}
12. Ambient temperature	$T_0 = 70$°C
13. Relative angular velocity of ring and housing	$\omega \in [0.2;\ 2.0]$ rad·s^{-1}

Figs. 13, 14, and 15 show the results of numerical simulations obtained after applying the developed model for the parameters defined in Tab. 1. The results include the simulation of the damper housing temperature, the average pressure in the oil film, and the minimum oil film height. It should be emphasized that our model assumes stabilization of the damper working conditions. Therefore, on the horizontal axis, we present the value of $\bar{\omega}$, which is the average absolute value of the angular velocity. More precisely, $\bar{\omega} = \frac{1}{t_1 - t_0}\int_{t_0}^{t_1} |\omega(t)|\, dt$, where $t_1 - t_0$ is the volatility period of the ω function.

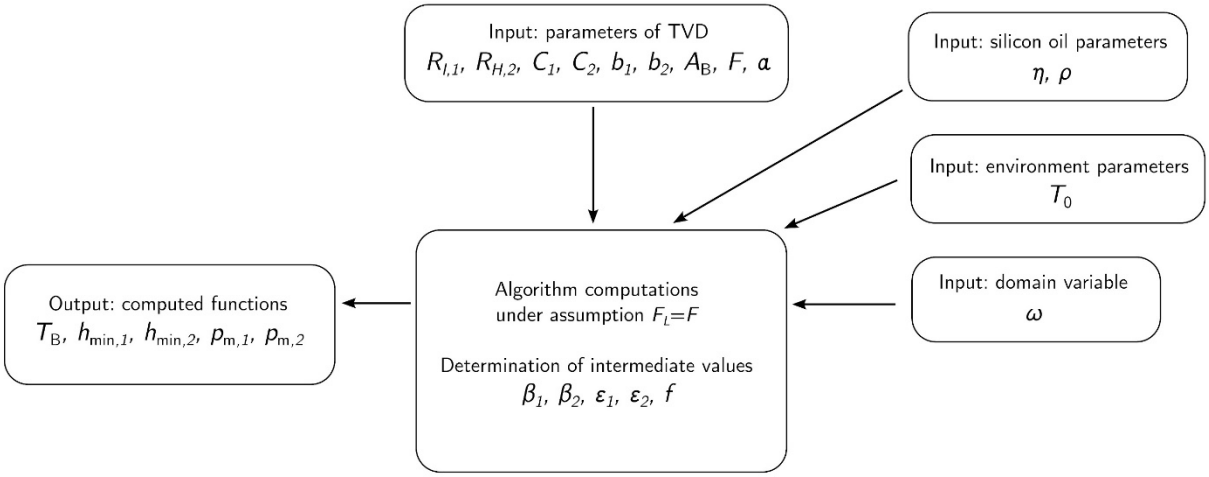

Fig. 12. Network diagram of an algorithm for solving the system of model equations

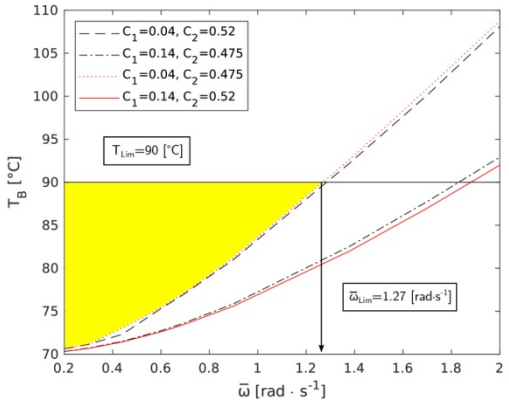

Fig. 13. Influence of the average absolute relative angular velocity on the damper operating temperature (the maximum average absolute relative angular velocity $\bar{\omega}_{Lim}$ is equal to 1.27 rad·s^{-1}and is achieved for the permissible temperature $T_{Lim} = 90°C$)

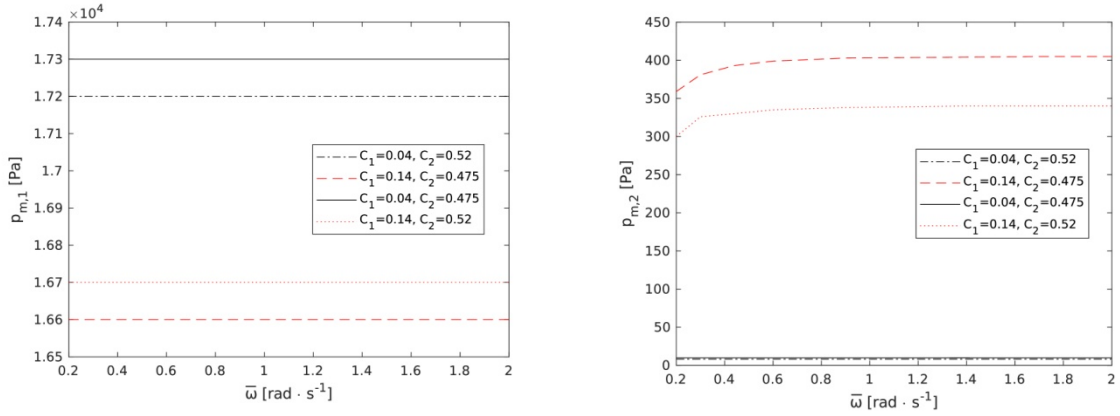

(a) (b)

Fig. 14. Influence of the average absolute relative angular velocity on the average pressure in (a) the inner oil film and (b) the outer oil film

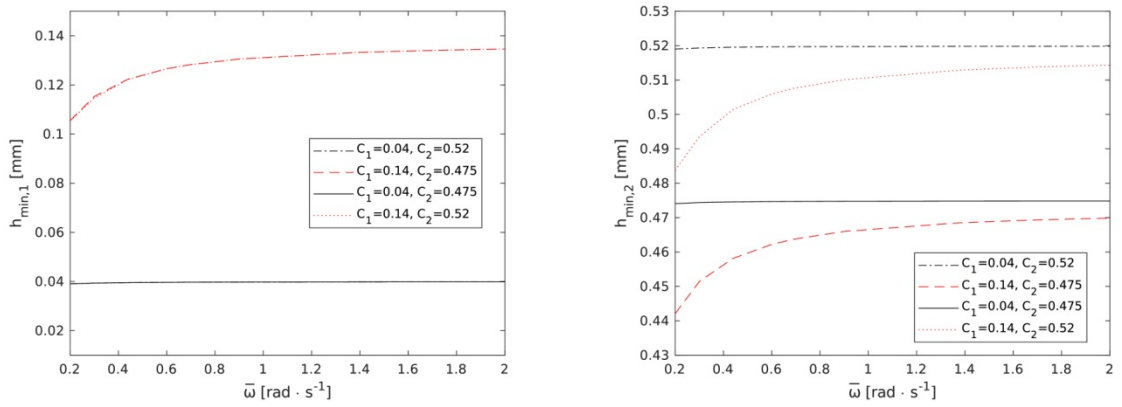

(a) (b)

Fig. 15. Influence of the average absolute relative angular velocity on (a) the inner minimum oil film thickness and (b) the outer minimum oil film thickness

6. CONCLUSIONS

Based on the results of the numerical simulations (Figs. 13, 14 and 15), the following conclusions can be drawn:

- with an increase in the internal radial clearance C_1, the operating temperature of the damper decreases,
- the permissible temperature T_{Lim} of the tested damper is reached at $\bar{\omega} = 1.2$ rad·s^{-1}, $C_1 = 0.04$ mm and $C_2 = 0.475$ mm,
- the minimum thickness of the oil film is slightly lower than the value of the radial clearances – this results in a location close to the concentric position inertia ring and housing,
- the pressure generated in the damper in the inner oil film is greater than the pressure in the outer oil film.

In summary, the torsional vibrations viscous dampers presented in the paper could work properly for the analyzed angular velocity and assumed radial clearances.

References

1. Atzori, B. & Berto, F. & Lazzarin, P. & Quaresimin, M. A stress invariant based criterion to estimate fatigue damage under multiaxial loading. *International Journal of Fatigue*. 2006. Vol. 28. P. 485-493.
2. Czarnigowski, J. & Drozdziel, P. & Kordos, P. Characteristic rotational speed ranges of a crankshaft during combustion engine operation at car maintenance. *Eksploatacjai Niezawodność - Maintenance and Reliability*. 2002. Vol. 2. No. 14. P. 55-62.
3. Becarra, J. & Jimenez, F. & Torrez, M. & Sanchez, D. & Carvajal, E. Failure analysis of reciprocating compressor crankshafts. *Engineering Failure Analysis*. 2011. Vol. 18. No. 2. P. 735-746.
4. Asi, O. Failure analysis of a crankshaft made from ductile cast iron. *Engineering Failure Analysis*. 2005. Vol. 13. No. 8. P. 1260-1267.
5. Alfares, M. & Falah, A. & Elkholy, A. Failure analysis of a vehicle engine crankshaft. *Journal of Failure Analysis and Prevention*. 2007. Vol. 7. No. 1. P. 12-17.
6. Bahumik, S. & Rangaraju, R. & Venkataswamy, M. & Baskaran, T. & Parameswara, M. Fatigue fracture of crankshaft of an aircraft engine. *Engineering Failure Analysis*. 2002. Vol. 9. No. 3. P. 255-263.

7. Changli, C. & Chengjie, Z. & Deping, W. Analysis of an unusual crankshaft failure. *Engineering Failure Analysis*. 2005. Vol. 12. No. 3. P. 465-473.
8. Fonte, M. & Li, B. & Reis, L. & Freitas, M. Crankshaft failure analysis of a motor vehicle. *Engineering Failure Analysis*. 2013. Vol. 35. P. 147-152.
9. Pandey, R. Failure of diesel engine crankshaft. *Engineering Failure Analysis*. 2003. Vol. 10. No. 2. P. 165-175.
10. Chen, X. & Yu, X. & Hu, R. & Li, J. Statistical distribution of crankshaft fatigue: Experiment and modelling. *Engineering Failure Analysis*. 2014. Vol. 4. P. 210-220.
11. Bue, L. & Stefano, A. & Giagonia, C. & Pipitone, E. Misfire Detection System based on the Measure of Crankshaft Angular Velocity. In: *Advanced Microsystems for Automotive Applications 2007*. Berlin, Heidelberg: Springer. 2007. P. 149-161.
12. Drozdziel, P. & Krzywonos, L. The estimation of the reliability of the first daily diesel engine start-up during its operation in the vehicle. *Eksploatacjai Niezawodność - Maintenance and Reliability*. 2009. Vol. 1. No. 41. P. 4-10.
13. Jung, D. & Kim, H. & Pyoun, Y. & Gafurov, A. & Choi, G. & Ahn, J. Reliability prediction of the fatigue life of a crankshaft. *Journal of Mechanical Science and Technology*. 2009. Vol. 23. P. 1071-1074.
14. Orczyk, M. & Tomaszewski, F. Diagnostic and reliability model of an internal combustion engine. *Combustion Engines*. 2020. Vol. 180. No. 1. P. 41-46.
15. Singh, S. & Abdullah, S. & Mohamed, N. Reliability analysis and prediction for time to failure distribution of an automobile crankshaft. *Eksploatacjai Niezawodność - Maintenance and Reliability*. 2015. Vol. 17. No. 3. P. 408-415.
16. Deuszkiewicz, P. & Pankiewicz, J. & Dziurdz, J. & Zawisza, M. Modeling of powertrain system dynamic behavior with torsional vibration damper. *Advanced Materials Research*. 2014. Vol. 1036. P. 586-591.
17. Kodama, T. & Honda, Y. Study on the Modeling and Dynamic Characteristics of the Viscous Damper Silicone Fluid Using Vibration Control of Engine Crankshaft Systems. *International Journal of Mechanical Engineering and Robotics Research*. 2018. Vol. 7. No. 3. P. 273-278.
18. Wilson, W. *Practical solution of torsional vibration problems*. New York: Springer. 1969.
19. Senjanović, I. & Hadžić, N. & Murawski, L. & Vladimir, N. & Alujević, N. & Cho, D.-S. Analytical procedures for torsional vibration analysis of ship power transmission system. *Engineering Structures*. 2019. Vol. 178. P. 227-244.
20. Mollenhauer, K. & Tschöke, H. *Handbook of diesel engines*. Berlin: Springer. 2010.
21. Nestorides, E. *A handbook on torsional vibration*. Cambridge: Cambridge University Press. 1958.
22. Homik, W. & Markowski, T. Temperature as a source of information about the technical condition viscous torsion damper. *Solid State Phenomena.* 2015. Vol. 236. P. 78-84.
23. Lakshminarayanan, P. & Agraval, A. *Design and development of heavy duty diesel engines: a handbook*. Singapore: Springer. 2020.
24. Latarche, M. *Pounder's Marine Diesel Engines and Gas Turbines*. Cambridge: Butterworth-Heinemann. 2021.
25. Wilbur, C. & Wight, D. *Pounder's Marine Diesel Engines*. Thetford, Norfolk: Butterworth. 1984.
26. Chmielowiec, A. & Michajłyszyn, A. & Homik, W. Behaviour of a torsional vibration viscous damper in the event of a damper fluid shortage. *Polish Maritime Research*. 2023. Vol. 30. No. 2. P. 105-113.
27. Homik, W. & Mazurkow, A. & Woś, P. Application of a thermo-hydrodynamic model of a viscous torsional vibration damper to determining its operating temperature in a steady state. *Materials*. 2021. Vol. 14. No. 18. Paper No. 5234. 14 p.
28. Zygmuntowicz, J. The development of the torsional vibration calculations program applied in H.Cegielski Company. In: *Proceedings of 23rd CIMAC Congress*. Hamburg. 2001. P. 9c-02.
29. DIN 31652. *Plain bearings - Hydrodynamic plain journal bearings under steady-state conditions*. Deutsches Institut fur Normung. 2017.
30. Barwell, F. *Bearing Systems: Principles and Practice*. Oxford: Oxford University Press. 1980.

31. Barwell, F. Theories of wear and their significance for engineering practice. *Treatise on Materials Science & Technology*. 1979. Vol. 13. P. 1-83.
32. Hori, Y. *Hydrodynamic Lubrication*. Tokyo: Springer-Verlag. 2006.
33. Kaniewski, W. Warunki brzegowe diatermicznego filmu smarnego. *Zeszyty naukowe Politechniki Łódzkiej Zeszyt specjalny*. 1977. Vol. 14(281). P. 7-22. [In Polish: Kaniewski, W. Boundary conditions of a diathermic lubricating film. *Scientific notebooks of the Lodz University of Technology. Special notebook*.]
34. Lund, J. Review of the concept of dynamic coefficients for fluid film journal bearings. *Journal of Tribology*. 1987. Vol. 109. P. 37-41.
35. Clearco Products Co. Inc. Available at: http://www.clearcoproducts.com.
36. Chmielowiec, A. & Woś, W. & Gumieniak, J. Viscosity approximation of PDMS using Weibull function. *Materials*. 2021. Vol. 14. No. 6060. 21 p.

Received 03.04.2022; accepted in revised form 30.11.2023